Continuous fluorescence microphotolysis of anthracene-labeled phospholipids in membranes

Theoretical approach of the simultaneous determination of their photodimerization and lateral diffusion rates

Xavier Ferrières,* André Lopez,‡ Anne Altibelli,‡ Laurence Dupou-Cezanne,‡
Jean-Louis Lagouanelle,* and Jean-François Tocanne‡

*Laboratoire Langage et Systèmes Informatiques, Unité associée au Centre National de ea Recherche Scientifique, Université Paul Sabatier, F-31062 Toulouse, France ‡Centre de Recherches de Biochimie et de Génétique cellulaires du Centre National de ea Recherche Scientifique, F-31062, Toulouse, France

ABSTRACT Anthracene is a fluorescent and photoactivatable (dimerization) group which can be used for investigating the lateral distribution and dynamics of lipids in membranes. In fluorescence recovery after photobleaching or in microphotolysis experiments, and when using this fluorophore, the bleaching (or microphotolysis) step in the illuminated part of the membrane is in fact the sum of two antagonistic processes: fluorescence decay, which is due to dimerization of anthracene residues, and fluorescence recovery, which is due to a diffusion mediated exchange of bleached and unbleached particles between the illuminated and diffusion area in the membrane. Here, we propose a new mathematical algorithm that enables such a second-order reaction-diffusion process to be analyzed. After coupling a fluorescence recovery step to a microphotolysis step, this algorithm allows us to calculate the lateral diffusion coefficient D and the photodimerization constant K of anthracene-labeled lipids in membranes, two parameters which contribute to the understanding of the fluidity of the lipid phase in membranes. This algorithm also provides us with a complete description of the anthracene-labeled molecules distribution in the illuminated and diffusion area, at any time of the experiment. The fluorescence recovery after microphotolysis procedure we propose was tested with an anthracene-labeled phosphatidylcholine inserted in egg-phosphatidylcholine multilayers, in monolayers adsorbed onto alkylated glass surfaces and in the plasma membrane of Chinese hamster ovary cells. It is shown that this procedure can also be used to evaluate the important parameters of probe mobile fraction and to determine the relative size of the illuminated and diffusion areas. This will enable membranes to be explored in terms of microdomains and/or macrodomains.

INTRODUCTION

It is now generally agreed that membrane lipid "fluidity" plays a key regulatory role in the functioning of membrane proteins (1). This complex parameter combines structural (lipid conformational and rotational motions) and diffusion aspects of the membrane lipid domain. It can be investigated using a large variety of techniques which, in a specific way, give information on one or another of these aspects. For example, and after labeling the lipid phase with an appropriate lipophilic fluorescent probe, the first aspect which is often referred to as membrane lipid "microviscosity" (2), can be investigated by means of fluorescence depolarization measurements, while the second can be studied via fluorescence recovery after photobleaching (FRAP) experiments (3, 5).

Nevertheless, it has been shown that changes in membrane lipid microviscosity are not necessarily correlated with changes in the lipid lateral diffusion rate (4). Therefore, it is important to describe the fluidity of lipids in membranes in its various aspects, i.e., conformational, rotational, and diffusional motions of lipid molecules.

Address all correspondence to Dr. Tocanne.

To investigate both the lateral distribution and motion of intrinsic lipids in membranes, we have developed a new photochemical technique using anthracene attached to a fatty acid as a photoactivatable group (6, 7). This hydrophobic group, which is well suited for labeling the hydrophobic core of the membrane (8–10), is fluorescent, but under illumination at 360 nm, it forms also 9-9′, 10-10′ covalently bound dimers, which are not fluorescent. Thus, after incorporation into membrane lipids, it can be used to (*a*) study the lateral distribution of lipids in membranes after photo-cross-linking of adjacent anthracene-labeled molecules and subsequent identification of the photodimers, (*b*) measure the lateral diffusion rate of the labeled molecules using a FRAP technique, (*c*) investigate the structure of the membrane lipid phase by measuring the dimerization constant k_d which characterizes the photodimerization reaction. Indeed regardless of photochemical aspects, k_d depends on the lateral mobility but also on the rotational and conformational motions of lipid molecules within the membrane.

9-(2-Anthryl)-nonanoic acid and various corresponding anthracene-phospholipids have been synthesized (6). Their physical and phase properties have also been investigated (6). The anthracene-fatty acid has been shown to

0006-3495/89/06/1081/11 $2.00

be incorporated at a high rate into the various membrane lipids of both prokaryotic (8) and eukaryotic (10) cells in culture. This provides us with the great advantage of being able to study, in situ, the phase behavior of constitutive membrane lipids. A simple and versatile photocross-linking method has been described for the determination of the lateral distribution of lipids in model and natural membranes (7, 9), which has been successfully applied to the bacterium *Micrococcus luteus* (9). A FRAP technique, well suited for the study of anthracene-labeled phospholipids has been developed (11). Combined with metabolic incorporation of the anthracene-fatty acid into membrane lipids, it has enabled the lateral diffusion rate of intrinsic lipids in the plasma membrane of living cells (Chinese hamster ovary cells) to be determined (12).

Here, we present a new approach which, through a single experiment, provides information about both the structural and diffusion terms that enter into the definition of the fluidity of the lipid phase in membranes. This approach uses anthracene-labeled lipid molecules. It is based on a spatial and temporal discretization combined with a new mathematical algorithm, which allows us to evaluate the diffusion coefficient D and the dimerization constant k_d of the probe molecules from the fluorescence signal that is obtained through fluorescence recovery after continuous fluorescence microphotolysis experiments. We also disclose some of the experimental difficulties that are inherent to this methodology of continuous fluorescence microphotolysis.

MATERIAL AND METHODS

Chemicals

n-Octadecyltrichlorosilane (Merck, Schuchardt, FRG, for synthesis) and *n*-hexadecane (Fluka AG, Buchs, Switzerland) were used without further purification. Synthesis of sn-1 -acyl-sn-2 -(9-[2-anthryl]- nonanoyl)—glycero-3 phosphocholine (EAPC) from egg yolk lysolecithin has been described previously (6). Egg yolk phosphatidylcholine (egg-PC) was obtained from Sigma Chemical Co., St. Louis, MO. 5-(*N*-hexadecanoyl)-aminofluorescein (HEDAF) was purchased from Molecular Probes, Eugene, Oregon. The purity of these compounds was checked by thin-layer chromatography. Salts and solvents were of analytical grade.

Lipid monolayers adsorbed on alkylated planar glass surfaces

Before being alkylated, glass coverslips (2.4 × 3.2 cm^2) were first washed in hot alkaline detergent solution for 30 min and sonicated 30 min (60°C) in a bath sonicator (80 KHz, heat ultrasonic system, Ultrasous Annemasse, Paris, France). After washing with distilled water, the glass slides were soaked overnight in chromic acid. Then they were rinsed with distilled water, sonicated for 15 min in 1 mM sodium hydroxide, rinsed again with distilled water, and finally dried, in vacuo in a dessicator in the presence of phosphoric anhydride.

Alkylated glass slides were obtained by immersion of the clean and dry coverslips into a 80% *n*-hexadecane, 12% carbon tetrachloride, 8% chloroform, and 0.1% octadecyltrichlorosilane solution (13). After 15 min reaction under gentle stirring, the glass slides were removed and then washed by immersion (three times) in chloroform. Alkylated coverslips were stored in a dry atmosphere and used within 5–10 d after preparation.

Adsorbed monolayers were prepared using a small trough (5 × 2.5 × 0.8 cm^3) milled from plexiglass. An alkylated coverslip was fixed to the edges of the trough, in order to cover the monolayer surface. The trough was filled with half the subphase volume required to fill it completely. Lipids were spread in the form of chloroform/methanol 1:1 (vol/vol) solution, and the surface pressure was raised to the desired value by stepwise addition of the lipids. After a 60 min period of stabilization, the monolayer was leveled off by addition of the second half of the subphase volume in order to bring the lipid monolayer and the alkylated glass surface into contact. Care was taken to avoid air bubbles between the glass and water surfaces.

Hydrated egg-PC multilayers

EAPC was added to egg-PC at a molar ratio of 0.5%. 2 mg of the lipid mixture in chloroform solution and were deposited on a microscope slide. The solvent was evaporated under reduced pressure. Lipids were hydrated by immersing the plate in distilled water for 10 min at room temperature.

Large domains of multilayers were obtained by pressing the hydrated lipids between the slide and a coverslip at a pressure of 60 N/cm^2 (14). The preparation was then sealed with paraffin wax to prevent dehydration, and stored at 4°C under a water saturated nitrogen atmosphere.

Membrane labeling by phospholipid exchange protein

Chinese Hamster Ovary (CHO) cells were obtained from Dr. Siminovitch, (Toronto, Canada). They are routinely grown in suspension at 37°C in Eagle's minimal essential medium (15) (MEM0111, Eurobio, Paris, France) supplemented by 6% fetal calf serum (Boehringer, Mannheim, FRG).

250 μl of degassed phosphate buffered saline (PBS: 0.15 M NaCl; 0.01 M Na_2HPO_4; 0.01 M KH_2PO_4; pH 7.2) were added to 150 μg of dry EAPC. The mixture was vortexed and sonicated (80 KHz) twice for 1 min. 250 μl of the sonicated lipid suspension were mixed with 1 ml of cell suspension (3 10^6 cells/ml); 100 μl of buffer containing the phospholipid exchange protein (500 μg/ml) purified from spinach leaves (16) were then added. Incubation was carried out for 15 min at 37°C. Then the cells were washed twice by centrifugation with 3 ml of PBS. A drop of the pellet was deposited between slide and coverslip.

Fluorescence recovery after continuous fluorescence microphotolysis experiments

Experiments were carried out under conditions of constant incident light intensity and uniform disk illumination, using an experimental set-up

based on a Leitz Ortholux II Fluorescence microscope, which has already been described (11).

RESULTS AND DISCUSSION

Theory

In FRAP experiments carried out with anthracene-labeled molecules, the bleaching step is in fact the sum of two antagonist processes. One, which corresponds to fluorescence decay, is due to the dimerization reaction of anthracene-labeled lipid molecules in the illuminated area and is characterized by the dimerization constant k_d. The other, which brings about fluorescence recovery, is due to the diffusion-mediated exchange of anthracene-lipid monomers and dimers between the illuminated and diffusion area and is characterized by the lateral diffusion coefficient D. When bleaching time is sufficiently long (the so-called condition of microphotolysis) and when using an appropriate modelization of the system, it is possible to estimate D and k_d from the fluorescence signal that originates from the illuminated area in the membrane. Such an approach also has the great advantage of overcoming the difficult problem of correctly describing the post-bleaching probe concentration profile in the illuminated area when FRAP experiments are carried out with highly mobile lipid molecules or with illuminated area of very small radius. Indeed, if fluorophore transport occurs between the illuminated and diffusion area in the membrane, during the bleaching step, and if this fact is ignored, then the D values obtained will be false.

Microphotolysis experiments corresponding to first-order reaction diffusion process have been already described by Peters et al. (17, 18). Nevertheless, the numerical methods they propose for the calculation of D (spatial discretization associated with spectral expansion, temporal discretization, and computation using the Crank-Nicholson integration scheme or a generalized moment expansion method), are valid only for first-order (or pseudo first-order) reaction. They cannot be easily used to solve the much more complicated case of a second-order reaction-diffusion process. In this case, the change with time in fluorophore concentration in the illuminated area is to be accounted for by a nonlinear differential equation (see Eq. [7]), for which there is no analytical solution and the resolution of which cannot be achieved by spectral or generalized moment expansions. This approach would either be impossible or much too complicated for use except in very particular cases. Here we show that spatial and temporal discretization of the system associated with quasilinearization of the operator coupled with an adequate mathematical algorithm allows correct description of a second-order reaction-diffusion process.

Photodimerization of anthracene

Photochemistry of anthracene and its derivatives can be summarized as follows:

$A + h\nu$ (340–380 nm)	$\rightarrow A^*$	Light absorption
A^*	$\rightarrow A + h\nu'$ (390–430 nm)	Fluorescence emission
$A^* + A$	$\rightarrow A_2$	Dimerization.

Anthracene absorbs light in the 240–290 nm and 340–380 nm regions. A fluorescence emission can be observed between 390 and 430 nm. Upon irradiation in the near ultra-violet (~360 nm), a dimerization reaction can also occur. As already stated, it leads, in an irreversible way, to 9-9', 10-10' covalently bound dimers which are not fluorescent (6, 7). These dimers are chemically very stable. Nevertheless, the dimerization reaction can be partly reversed by illuminating the dimers at ~260–280 nm (7). This property is used in the photo-cross-linking method we propose for investigating the lateral distribution of lipids in membranes (7). Note also that upon irradiation, side photo-products such as photo-oxides can eventually be formed and interfere with the dimerization reaction (7). In fact, both in model and natural membranes, where anthracene derivatives are relatively highly concentrated and in a well organized phase, the photo-dimerization reaction proceeds at a much higher rate than the photo-oxidation reaction. We never detected photo-oxides in our photo-dimerization experiments (7). Therefore, the dimerization reaction is the sole to be considered. This is a strict second order process which, in the close reactor a membrane bilayer is, can be written as:

$$2dC/dt = -k_d C^* C_g, \quad (1)$$

where C^* and C_g are the concentrations of the anthracene residues in the excited and ground state respectively and k_d is the dimerization constant.

In condition of constant illumination and because the excited life-time of anthracene is very short (τ = 4 ns) (19) as compared with the time-scale (1–2 s) of a microphotolysis experiment, the concentration of molecules in the excited state is proportional to the excitation light intensity I_{ex} and to the total concentration C of fluorophores (steady state concentration of excited molecules):

$$C^* = \alpha I_{ex} C \quad (2)$$

and the concentration C_g of molecules which, after excitation, remain in the ground state is:

$$C_g = (1 - \alpha I_{ex})\, C. \quad (3)$$

Eq. 1 can be written as:

$$dC/dt = -\tfrac{1}{2}k_d\alpha I_{ex}(1 - \alpha I_{ex})\, C^2. \quad (4)$$

Due to the loss of conjugation between the aromatic rings, the anthracene dimers that are formed are not fluorescent. Therefore, the fluorescence signal originating from the reactor, can be used to monitor the dimerization reaction. The anthracene residues in the excited state split into two populations: those that give fluorescence and those that lead to photodimers. The splitting ratio between these two populations depends on both photochemical and structural factors, but is constant for given reaction conditions.

This means that the intensity I_f of the observed fluorescence signal is strictly proportional to the number of molecules in the excited state:

$$I_f = \gamma C^* = \gamma\alpha I_{ex} C. \quad (5)$$

In these conditions, Eq. 4 converts to:

$$dI_f/dt = \tfrac{1}{2}[k_d/\gamma](1 - \alpha I_{ex})\,(I_f)^2 = -K(I_f)^2 \quad (6)$$

in which $K = \tfrac{1}{2}[k_d/\gamma]\,(1 - \alpha I_{ex})$.

This equation clearly shows that the apparent dimerization constant K, which can be inferred from the kinetics of the fluorescence decay, still depends on excitation conditions. Note that the above derivation is valid only for conditions of low or moderate excitation light intensity I_{ex} (no fluorescence saturation) and low probe concentration in the membrane lipid phase (absence of radiative or resonance fluorescence energy transfer).

In what follows and for the sake of clarity, we will refer only to the apparent constant K, which, for given experimental conditions, is a characteristic of the system under investigation.

Photodimerization-diffusion process

When coupling a diffusional process to the photodimerization reaction, the time development of the concentration $C(x, t)$ of nondimerized fluorophores is now described, at time t and spatial point x, by the general dimerization-diffusion equation:

$$\frac{\partial C(x, t)}{\partial t} = D1(x)C(x, t) - k(x)C^2(x, t), \quad (7)$$

in which $D \cdot 1(x)$ is the linear differential diffusion operator, and $k(x)$ is a function associated with the scalar dimerization constant.

The initial distribution of the fluorophore molecules is supposed to be homogeneous in the membrane plane.

$$C(x, 0) = C_0.$$

For a flat membrane, a circular illuminated area of radius r_i and an isotropic diffusion, the distribution of fluorophores in the membrane plane is axialy symmetric and can be studied in a circular diffusion area of radius R. The ratio R/r_i is taken large enough to satisfy the condition of infinite reservoir (11, 20).

In these conditions, Eq. 7 is described using cylindrical coordinates by

$$\frac{\partial C(r, t)}{\partial t} = D\left(\frac{\partial^2}{\partial r^2} + \frac{1}{r}\frac{\partial}{\partial r}\right)C(r, t) - k(r)C^2(r, t), \quad (8)$$

in which $C(r, t)$ is the surfacic concentration of the diffusing species at distance r from the origin (illuminated area center) and at time t. For a complete definition of the problem, the boundary conditions of probe concentration are:

$$C(., 0) = C_0, \quad C(R, .) = C_0, \quad \text{and} \quad \frac{\partial C(0, .)}{\partial r} = 0.$$

In conditions of uniform disk illumination, the excitation light intensity profile has a rectangular shape (11). As seen in the preceding section, the dimerization reaction linearly depends on I_{ex}. Because the excited state life-time of anthracene is very short (τ = 4 ns) (19), as compared with the kinetics of diffusion, the dimerization reaction will occur only in the illuminated area:

$$k(r) = \tfrac{1}{2}k_d\alpha I_{ex}(1 - \alpha I_{ex})H(r_i - r),$$

in which $H(r_i - r)$ is the Heaviside function defined by:

$$H(r_i - r) = 1 \text{ for } r \le r_i \text{ and } H(r_i - r) = 0 \text{ for } r > r_i.$$

As indicated above, the photodimerization-diffusion process can be monitored by the measurement of the fluorescence intensity originating from the illuminated area:

$$i(r, t) = \gamma\alpha I_{ex} C(r, t).$$

This leads to the new equation:

$$\frac{\partial i(r, t)}{\partial t} = D\left(\frac{\partial^2}{\partial r^2} + \frac{1}{r}\frac{\partial}{\partial r}\right)i(r, t) - K(r)i^2(r, t) \quad (9)$$

with:

$$i(., 0) = I_0, \quad i(R, .) = I_0, \quad \frac{\partial i(0, .)}{\partial r} = 0,$$

and

$$K(r) = k(r)/[\gamma(\alpha I_{ex})] = KH(r_i - r),$$

in which K has its above meaning. (See above.)

In fact, we have already shown that the light intensity profile is not strictly rectangular but is slightly trapezoi-

dal in shape (11). It is therefore more realistic to use, not the Heaviside function but a continuously differentiable function $h(r)$ such as $h(r_i) = 1/2$.

Inverse problem

The fluorescence intensity, which originates at time t from the entire illuminated area, can be calculated by:

$$I(t) = 2\pi \int_0^{r_1} i(r, t)\, r\, dr. \tag{10}$$

Let $I_f(t)$ be the corresponding experimental value.

The inverse problem which we have to solve (21) is then to determine the solutions D_{sol} and K_{sol} for D and K so that Eq. 9 accounts as well as possible for the process observed.

Minimization method

For this purpose, we define the quadratic function:

$$g(D, K) = \sum_{j=1}^{N} [I(D, K, t_j) - I_f(t_j)]^2, \tag{11}$$

where $(t_1, t_2, \ldots, t_N)$ corresponds to a given time sampling. We have to search its minimum value, and a necessary condition to obtain the minimum is:

$$g'(D_{sol}, K_{sol}) = 0. \tag{12}$$

To approach this condition, we use the Gauss-Newton iterative method defined by:

$$x_{p+1} = x_p - [f'^t(x_p) \cdot f'(x_p)]^{-1} \cdot g'(x_p), \tag{13}$$

in which $x_p = (D_p, K_p)$, corresponds to the pth values of D and K. With the same notation, x_0 corresponds to the initial K_0 and D_0 values used for the initialization of the iterative process.

f'^t is the maximal rank matrix:

$$\begin{bmatrix} \frac{\partial I(t_1)}{\partial D} & \frac{\partial I(t_2)}{\partial D} & \cdots\cdots & \frac{\partial I(t_N)}{\partial D} \\ \frac{\partial I(t_1)}{\partial K} & \frac{\partial I(t_2)}{\partial K} & \cdots\cdots & \frac{\partial I(t_N)}{\partial K} \end{bmatrix}. \tag{14}$$

The numerical computation of the partial derivatives by a finite differences method is unstable and time consuming. They were obtained here in an elegant way from Eqs. 9 and 10 using the following argument from Eq. 10, we can write, with a minimum of regularity:

$$\frac{\partial I(t)}{\partial D} = 2\pi \int_0^{r_1} \frac{\partial i(D, K, r, t)}{\partial D}\, r\, dr \tag{15}$$

$$\frac{\partial I(t)}{\partial K} = 2\pi \int_0^{r_1} \frac{\partial i(D, K, r, t)}{\partial K}\, r\, dr. \tag{16}$$

Letting $u = \partial i/\partial D$ and $v = \partial i/\partial K$ it can be shown that:

$$\frac{\partial u}{\partial t} - D\, l(r)\, u + 2\, k'(r)\, i\, u = 1(i) \tag{17.1}$$

with $u(., 0) = 0$, and $[\partial u(0, .)]/\partial r = u(R, .) = 0$

$$\frac{\partial v}{\partial t} - D\, l(r)\, v + 2\, k'(r)\, iv = -k(r)\, i^2 \tag{17.2}$$

with $v(., 0) = 0$, and $[\partial v(r, .)]/\partial r = v(R, .) = 0$.

These parabolic equations are linear and associated with the same operator, and have the same initial and boundary conditions. They can be solved simultaneously when $i(r, t)$ is known (Eq. 9).

Resolution of the nonlinear equation

This is a crucial step in the numerical process (22). Eq. 9 is solved iteratively by a quasi-Newton method:

$$\frac{\partial i_{n+1}(r, t)}{\partial t} = D\, l(r) i_{n+1}(r, t) - 2k'(r) i_n(r, t)\, i_{n+1}(r, t) + k'(r) i_n^2(r, t) \tag{18}$$

with $i_{n+1}(., 0) = I_0$, $[\partial i_{n+1}(0, .)]/\partial r = 0$, $i_{n+1}(R, .) = I_0$, in which $i_n(r, t)$ has been already determined and $i_0(r, t) = I_0$.

Then, we have to solve a linear parabolic equation to obtain $i_{n+1}(r, t)$. The discretization method used is the Crank-Nicholson scheme associated with a finite difference method and a variable spatial step.

Algorithm

Finally, the different steps required to obtain the optimal coefficients D_{sol} and K_{sol} can be summarized in the following algorithm. (*a*) Initialize the process; choose D_0, K_0, and evaluate $g(D_0, K_0)$. (*b*) Solve Eq. 9, calculate $I(t)$. (*c*) Solve Eq. 11 to obtain the derivatives. (*d*) Calculate D_{p+1}, K_{p+1} from Eq. 13 and evaluate $g(D_{p+1}, K_{p+1})$. (*e*) Go to *b* until convergence.

Stray-light background signal

We have seen that in its principle, a fluorescence microphotolysis experiment is relatively simply. Furthermore, fluorescence can be used as a sensitive and specific technique to determine the number of fluorophore molecules that are present at any time in the illuminated area of the membrane. In the above description of the photodimerization-diffusion process, the emitted fluorescence intensity was supposed to be directly proportional to the anthracene concentration. This means that, when illumi-

nating the membrane in the absence of probe, the photocurrent from the photomultiplier tube should be equal to zero. Actually, this did not appear to be the case. A stray-light signal is always observed in any fluorescence microscope (23), which is primarily due to light reflection phenomena and to the very epi-configuration (ploem system) which does not allow complete discrimination between the fluorescence excitation and emission beams.

This signal can be reduced but not suppressed by the interposition of a field diaphragm in the emission beam just in front of the photomultiplier tube, in the conjugated image plane (11, 24). Therefore, the observed fluorescence intensity is not to be accounted for by a linear function but by an affine mathematical function which is to be introduced in any mathematical model.

In ordinary FRAP experiments, this problem can be ignored because the fluorescence recovery process is analyzed in terms of fractional recovered fluorescence intensities $f(t)$:

$$f(t) = \frac{I_f(t) - I_1}{I_0 - I_1},$$

in which I_0, I_1 are the absolute measured fluorescence intensities at the beginning and the end of the bleaching step respectively while $I_f(t)$ is that measured at any time of the recovery process.

In fluorescence microphotolysis experiments, interpretation of the data cannot be achieved by means of relative fluorescence intensities but requires the use of absolute values. The stray-light background signal (β or B) is nearly impossible to estimate in presence of the fluorophore. Its determination in parallel experiments can be risky. Therefore, we have introduced component B as a new parameter to be estimated together with K and D.

The fluorescence intensity is now written as:

$$i(r, t) = \gamma \alpha I_{ex} C(r, t) + \beta \tag{19}$$

and after integration over the illuminated area:

$$I_f(t) = I(t) + B, \tag{20}$$

in which $B = \beta \pi r_i^2$, and $I(t)$ is the absolute value of the fluorescence intensity.

Let $Q(r, t) = \gamma \alpha I_{ex} C(r, t)$.

Eq. 8 becomes:

$$\frac{\partial Q(r, t)}{\partial t} = D\, 1(r)\, Q(r, t) - K\, H(r_i - r)\, Q^2(r, t) \tag{21}$$

with $Q(., 0) = i_0 - \beta$, $[\partial Q(0, .)]/\partial r = 0$, $Q(R, t) = i_0 - \beta$ where $i_0 = [I_f(0)]/\pi r_i^2$.

Then we have to estimate the values D_{sol}, K_{sol}, B_{sol} of the D, K, B parameters for which the quadratic function is minimum:

$$g(D, K, B) = \sum_{j=1}^{N} [Q(D, K, B, t_j) - I_f(t_j) + B]^2. \tag{22}$$

In step 2 of the algorithm, we need the derivative $\partial Q/\partial B$. It is obtained, by solving a linear equation with the same operator as above.

Let $w = \partial Q/\partial B$, then we have:

$$\frac{\partial w}{\partial t} - D\, 1(r)\, w + 2\, K\, H(r_i - r)\, Q\, w = 0 \tag{23.1}$$

with the boundary conditions:

$$w(., 0) = -1, \quad \frac{\partial w(0, .)}{\partial r} = 0, \quad w(R, .) = -1. \tag{23.2}$$

Fluorescence recovery after microphotolysis experiments

In principle, fitting experimental fluorescence microphotolysis data with Eq. 21 and the algorithm we have developed would enable the three coefficients D, K, and B to be evaluated. However, preliminary experiments carried out with EAPC in egg-PC monolayers and multilayers showed that was not the case. Computations did not appear to be convergent, whatever the experimental conditions of excitation light intensity I_{ex}, illuminated area radius r_i and microphotolysis duration.

This difficulty was easily overcome by coupling a fluorescence recovery step to microphotolysis. Experiments were carried out in condition of constant illumination light intensity and were operated as follows. During the microphotolysis step, fluorescence from the illuminated area was continuously recorded. On the other hand, for the recovery step, fluorescence was stepwise recorded (9 steps) by flashing the lipid sample for a brief period of time (5 ms) after regular intervals of time in the dark. The microphotolysis step was analyzed using Eq. 21. Under the experimental conditions used, the recovery step can be considered as a pure diffusion process and was computed using the first right-hand term of Eq. 21. Very stable numerical solutions were obtained by this mean and hereafter, this type of experiments will be referred to as fluorescence recovery after microphotolysis or FRAM experiments, and the algorithm we have developed for their interpretation as the FRAM algorithm. Potentialities of this approach were tested with EAPC incorporated in egg-PC monolayers and multilayers and in the plasma membrane of CHO cells.

Fig. 1 shows typical FRAM data (+) obtained for EAPC incorporated at a concentration of 0.5% in egg-PC multilayers. The radius r_i of the illuminated area was 4.2

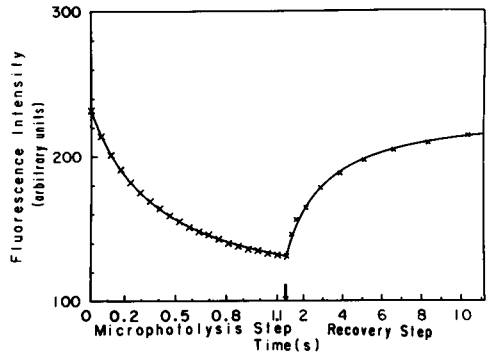

FIGURE 1 Experimental and calculated fluorescence recovery after microphotolysis curves. Experimental data (×) refers to a FRAM experiment carried out with EAPC at a concentration of 0.5% in egg-phosphatidylcholine multilayers. The radius r_i of the illuminated area was 4.2 μm. A large multilayer domain was selected ($R \simeq 50\ \mu$m) in order to work in conditions of infinite reservoir. Nine fluorescence recoveries were measured. Fluorescence intensities shown in the microphotolysis step are a selection of only a few out of those that were continuously recorded and stored in the microcomputer. The solid line is the best curve which could be calculated using the FRAM algorithm. It accounts for coefficients $D = 3.59 \cdot 10^{-8}$ cm^2/s, K = 0.514 (arbitrary units) and $B = 0.477$ (10% of the initial fluorescence intensity at time $t = 0$, see Table 1). Note that for the sake of clarity, the time-scale corresponding to the microphotolysis step was enlarged by a factor of 10. Arrow indicates the boundary of the two scales.

μm and the microphotolysis time was 1.16 s. The full line was the best curve that could be calculated using the FRAM algorithm. As shown in Table 1, it was obtained with a standard deviation of 0.12 (% of the initial fluorescence intensity, I_0) which was very close to the experimental error (0.11). This curve accounted for a diffusion coefficient $D = 3.59\ 10^{-8}$ cm^2/s which is close to the value of $3.53\ 10^{-8}$ cm^2/s which we have recently reported for the same probe in the same membrane model system, using conventional FRAP experiments (11). These values are close to that reported for similar systems (3, 14). The stray-light component B was estimated to 0.477 (arbitrary units). This value corresponded to $\simeq$10% of the initial fluorescence intensity I_0 and was close to the average value of 0.465 found in independent experiments for probe-free egg-PC multilayers. The dimerization constant K, was estimated to 0.104 (arbitrary units) in this system. It will be discussed together with K values obtained for monolayers and CHO plasma membranes.

It should be noted that the above experiments were carried out using a moderate intensity for the excitation light I_{ex}. Increasing I_{ex} led to a nonlinear relationship between the measured fluorescence intensity and probe concentration, with a loss of fluorescence. This might be due to fluorescence energy transfer processes between excited and nonexcited fluorophores (there is an overlap between the excitation and emission spectra of anthracene derivatives [6]), which is favored in multilayer systems where a large number of lipid bilayers are stacked over each other.

FRAM experiments were also carried out with monolayers adsorbed onto alkylated glass surfaces, which provide an interesting membrane model system (25) well suited for FRAP experiments. EAPC was added at a concentration of 1% to egg-PC and the monolayer, at the air-water interface, was compressed at a surface pressure $\pi = 30$ mN $\cdot$ m^{-1} before being adsorbed onto the alkylated glass. The radius of the illuminated area was $r_i = 8.75\ \mu$m and the microphotolysis time was 1.16 s. Fitting the experimental data with the FRAM algorithm ($\sigma = 0.22$) led to a diffusion coefficient $D = 1.48\ 10^{-8}$ cm^2/s that compared well with the value of $2 \cdot 10^{-8}$ cm^2/s reported for similar systems (26). A stray-light component $B = 0.127$ (arbitrary units) was found, which in this case, accounted to $\simeq$20% of I_0. This value was similar to

TABLE 1 Fluorescence recovery after microphotolysis data for EAPC in various membrane systems

Membrane systems	FRAM data			Reference parameters	
	D	K	B % I_0	B measured	D literature
Egg-phosphatidylcholine multilayers	3.59 ± 0.27	0.104 ± 0.002 σ = 0.12	0.477 ± 0.018 (10.7%)	0.465 ± 0.015	3.53 (11)
Egg-phosphatidylcholine adsorbed monolayers	1.48 ± 0.33	17.7 ± 1.6 σ = 0.22	0.127 ± 0.008 (20%)	0.13 ± 0.01	2 (26)
Chinese hamster ovary cell plasma membranes	0.21 ± 0.02	0.23 ± 0.02 σ = 0.23	2.9 ± 0.08 (22%)	3.4 ± 0.6	0.125 (12)
	0.15 ± 0.07	0.25 ± 0.01 σ = 0.1	3.7 ± 0.18 (19%)		

This table shows the lateral diffusion coefficient D (10^{-8} cm^2/s), the photodimerization constant K (arbitrary units) and the stray-light component B (arbitrary units and % I_0) calculated for EAPC from FRAM experiments. For comparison, experimentally measured B coefficients and D reference values from literature are also shown. The standard deviation is given as % of the initial fluorescence intensity I_0. It has to be compared to an experimental error evaluated to 0.11% of I_0 (11).

the average value of 0.13 found in parallel experiments for EAPC-free adsorbed egg-PC monolayers.

In the case of CHO cells, the plasma membrane was labeled with EAPC by means of a phospholipid exchange protein. The radius of the illuminated area was r_i = 1.95 μm and the microphotolysis time was 1.16 s. Data shown in Table 1 concern only two cells, simply to illustrate the quality of FRAM experiments on biological membranes. The measured diffusion coefficients were $D = 2.1 \cdot 10^{-9}$ cm^2/s (σ = 0.23) on one cell and $D = 1.5 \cdot 10^{-9}$ cm^2/s (σ = 0.1) on the other cell. They were close to the value of $1.25 \cdot 10^{-9}$ cm^2/s recently reported for EAPC-labeled CHO cells, using a FRAP technique (12). Note that the diffusion coefficient of $1.25 \cdot 10^{-9}$ cm^2/s is a mean D value representative of a collection of at least 50 cells (12) and that within a given cell population, a certain dispersion in D values exists (27, 28).

For the cellular membranes, the calculated stray-light components B (2.9, 3.7 in arbitrary units) accounted for ~20% of the initial fluorescence intensity I_0 and were similar to those measured in parallel experiments on nonlabeled cells.

With respect to the photodimerization constants K, the situation appeared to be somewhat more complicated. It is out of the scope of this paper to enter into a detailed analysis of this parameter. Nevertheless, it is worth stressing that K is the product of at least two contributions, a "spectroscopic" one and a "structural" one (29, 30). The structural part is to be related to the rotational and translational motions of the anthracene residues within the membrane. The spectroscopic component depends on the photochemical properties of the probe molecules, but also, as shown in the Theory section, upon the excitation light intensity I_{ex} and the apparatus functions (α and γ parameters). These parameters vary from one membrane system to the other. In the present approach, no attempt was made to quantify these parameters and, for that reason, calculated K values shown in Table 1 are given in arbitrary units. This explains the rather large dispersion which is observed in K values from one membrane system to the other and why comparison between those different values are difficult to achieve. Nevertheless, for fixed experimental conditions, comparison between relative K values is straightforward (25). In this respect, note the similarity between the K values measured for the CHO cells.

A complete analysis of the various contributions to K and normalization of this parameter by reference to a well defined reference system is currently under investigation in our laboratory.

The very close agreement for the three membrane systems tested, between the FRAM and FRAP diffusion coefficients D on the one hand, and the calculated and experimental stray-light components B on the other hand, demonstrates the validity of the FRAM approach for the determination of the two parameters D and K which enter into the definition of the photodimerization-diffusion process in the illuminated part of the membrane. This contention is also supported by the very close way experimental data fit when using the FRAM algorithm, as examplified in Fig. 1. For the various experiments reported (Table 1), the standard deviation was close to the experimental error.

Another advantage of the FRAM approach is to provide us with a complete description of the probe concentration in the illuminated and diffusion area, at any time of the photodimerization-diffusion process. This overcomes the complication which can sometimes arise in FRAP experiments for the computation of D from the fluorescence recovery data, because of a poor adequation between the mathematical model used and the actual post-bleaching probe concentration profile in the illuminated area (11). This is illustrated in Fig. 2 where we compare simulated FRAM experiments using the FRAM algorithm (*solid lines*) and FRAP curves (*dotted lines*). The latter were calculated using the numerical method we have recently developed to account for FRAP experiments in conditions of "uniform disk illumination" (11) and assuming that square-well probe concentration profiles still existed at the end of the microphotolysis steps. As can be seen, the two approaches lead to different recovery curves and the longer the microphotolysis step, the larger the difference between the two types of curves.

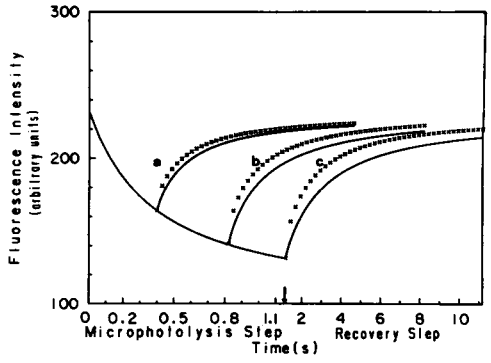

FIGURE 2 Numerical simulation of fluorescence recoveries after microphotolysis steps differing in time. (*a*) = 0.4 s; (*b*) = 0.8 s; (*c*) = 1.16 s. The solid line was calculated using the FRAM algorithm. The dotted line was calculated using the numerical method we have recently developed for the analysis of FRAP experiments (11) and assuming a square-well probe concentration profile at the end of the bleaching step. Parameters used in these computations were: $D = 3.59 \cdot 10^{-8}$ cm^2/s; K = 0.514 (arbitrary units); r_i = 4.2 μm; R = 19.74 μm. Note that for the sake of clarity, the time-scale part corresponding to the microphotolysis step was enlarged by a factor of 10 and that, strictly speaking, the time-scale shown relates to the sole curve (*c*). Curves *a* and *b* were drawn using the same procedure, with time-scale expansion over the first 0.4 and 0.8 s, respectively.

Probe concentration profiles in the illuminated and diffusion area, at the end of each microphotolysis step, were also calculated by means of the FRAM algorithm. As shown in Fig. 3, these profiles tended to differ more and more from a square-well profile for increasing microphotolysis time.

Finally another important parameter which can be inferred from FRAP experiments is the probe mobile fraction M. This parameter gives information on whether all the probe molecules are free to diffuse ($M = 100\%$) or whether part of them are immobilized in the membrane plane ($M < 100\%$). Note that an apparent immobile fraction can also be observed in cases where the diffusion area has a finite size, with a radius R not very large compared with the radius r_i of the illuminated area. We have recently discussed this point in detail and developed a numerical approach which enables the three parameters D, M, and R to be evaluated from FRAP experiments (11). Finite size of the diffusion area has also been recently accounted for in the interpretation of FRAP experiments carried out on axon hillock of nerve cell (31). In addition to D, the FRAM procedure and the FRAM algorithm we present here also allow us to calculate M and R. This is illustrated in Fig. 4 where simulated FRAM experiments, for different conditions of probe mobile fraction M and relative size of the radius r_i and R of the illuminated and diffusion area, are compared. As can be seen, the simulated curve (o) in conditions of 100% mobile fraction and finite-size reservoir ($R = 2r_i$) differed

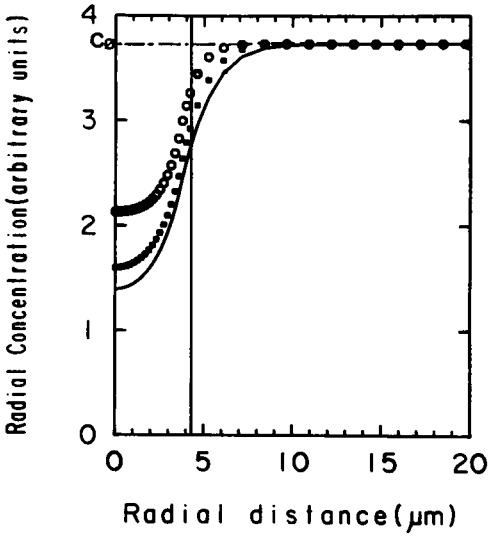

FIGURE 3 Numerical simulation by means of the FRAM algorithm of the radial probe concentration profiles in the illuminated and diffusion areas after various microphotolysis times, (*open circles*) = 0.4 s; (*filled squares*) = 0.8 s; (*solid lines*) = 1.16 s. The parameters used in these computations were $D = 3.59 \cdot 10^{-8}$ cm^2/s; K = 0.514 (arbitrary units); $r_i = 4.2$ μm; $R = 19.74$ μm.

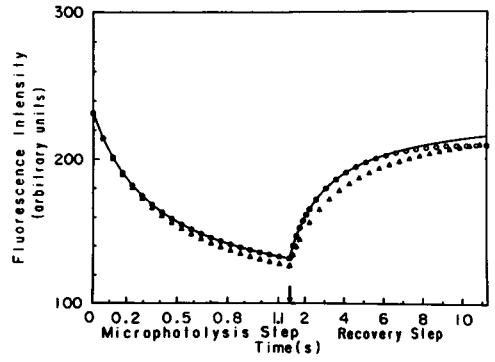

FIGURE 4 Numerical simulation, by means of the FRAM algorithm, of fluorescence recovery after microphotolysis curves for various conditions of probe mobile fraction M and relative size of the illuminated and diffusion area radius r_i and R. The parameters used in these computations were $D = 3.59 \cdot 10^{-8}$ cm^2/s; $K = 0.514$ (arbitrary units); $r_i = 4.2$ μm. (*Solid lines*): $M = 100\%$, $R = 19.74$ μm (the probe molecules are mobile in conditions of infinite reservoir). (*Open circles*) $M = 100\%$, $R = 2r_i = 8.2$ μm (the probe molecules are mobile in conditions of noninfinite reservoir). (*Open triangle*) $M = 70\%$, $R = 19.74$ μm (conditions of infinite reservoir and probe immobile fraction). Note the time-scale expansion in the microphotolysis step as in Figs. 1 and 2.

from the reference curve ($M = 100\%$, $R \gg r_i$) (—), only at the end of the recovery process. In contrast, the curve (Δ) that accounts for an immobile fraction ($M = 70\%$) with an infinite reservoir ($R \gg r_i$) differed from the reference curve both in the microphotolysis and recovery steps. This would make the discrimination between the conditions of probe immobile fraction and finite-size reservoir easier with FRAM than with FRAP experiments.

CONCLUSION

The FRAM procedure and the FRAM algorithm we have presented enable second-order reaction-diffusion processes to be studied in membranes. When using anthracene as a fluorescent and photoactivatable group, it is clear that FRAM experiments contain more information than FRAP or single microphotolysis experiments. Indeed, from a FRAM experiment, it is possible to extract the two kinetic parameters D and K, which characterize the dynamic behavior of anthracene-labeled lipids in membranes, and which both contribute to a more complete description of the membrane fluidity.

The FRAM algorithm can be used with any microcomputer. Typically, computation of the three parameters D, K, and B from one FRAM experiment took ~5 min with an OP.AT microcomputer (Normerel, Paris, France). This algorithm provides us with a complete description of the probe distribution in the illuminated and diffusion area, at any time of the experiment. It can also be used to

evaluate the important parameter of probe mobile fraction M and to determine the relative radius of the illuminated and diffusion area. This will enable membranes to be explored in terms of microdomains and/or macro-domains.

We would like to thank Dr. J. Noailles for fruitful discussions and Mr. J. Robb for rereading the English manuscript.

Received for publication 25 October 1988 and in final form 27 February 1989.

REFERENCES

1. Shinitzky, M., 1984. Membrane fluidity and cellular functions. *In* Physiology of Membrane Fluidity. M. Shinitzky, editor. CRC Press, Boca Raton, FL. 1:1–52.
2. Van der Meer, W. 1984. Physical aspects of membrane fluidity. *In* Physiology of Membrane Fluidity. M. Shinitzky, editor. CRC Press, Boca Raton, FL. 1:53–71.
3. Vaz, W. L. C., Z. I. Derzko, and K. A. Jacobson. 1982. Photobleaching measurements of the lateral diffusion of lipids and proteins in artificial phospholipid bilayer membranes. *Cell Surf. Rev.* 8:83–135.
4. Kleinfeld A. M., P. Dragsten, R. D. Klausner, W. J. Pjura, and E. D. Matayoshi. 1981. The lack of relationship between fluorescence polarization and lateral diffusion in biological membranes. *Biochim. Biophys. Acta.* 649:471–480.
5. Jacobson, K., E. Elson, D. Koppel, and W. Webb. 1983. International workshop on the application of fluorescence photobleaching techniques to problems in cell biology. *Fed. Proc.* 42:72–79.
6. de Bony, J., and J. F. Tocanne. 1983. Synthesis and physical properties of phosphatidylcholine labelled with 9-(2-anthryl)-nonanoic acid, a new fluorescent probe. *Chem. Phys. Lipids.* 32:105–121.
7. de Bony, J., and J. F. Tocanne. 1984. Photo-induced dimerization of anthracene-phospholipids for the study of the lateral distribution of lipids in membranes. *Eur. J. Biochem.* 143:373–379.
8. Welby, M., and J. F. Tocanne. 1982. Evidence for the incorporation of a fluorescent anthracene fatty acid into the membrane lipids of Micrococcus luteus. *Biochim. Biophys. Acta.* 689:173–176.
9. de Bony, J., G. Martin, M. Welby, and J. F. Tocanne. 1984. Evidence for a homogeneous lateral distribution of lipids in a bacterial membrane. *FEBS (Fed. Eur. Biochem. Soc.) Lett.* 174:1–6.
10. Dupou, L., J. Teissié, and J. F. Tocanne. 1986. Metabolic incorporation of 9-(2-anthryl)-nonanoic acid, new fluorescent and photoactivable probe, into the membrane lipids of Chinese hamster ovary cells. *Eur. J. Biochem.* 154:171–177.
11. Lopez, A., L. Dupou, A. Altibelli, J. Trotard, and J. F. Tocanne. 1988. Fluorescence recovery after photobleaching (FRAP) experiments under conditions of uniform disk illumination. Critical comparison of analytical solutions, and a new mathematical method for calculation of diffusion coefficient D. *Biophys. J.* 53:963–970.
12. Dupou, L., A. Lopez, and J. F. Tocanne. 1988. Comparative study of the lateral motion of extrinsic probes and anthracene-labelled constitutive phospholipids in the plasma membrane of Chinese hamster ovary cells. *Eur. J. Biochem.* 171:669–674.
13. Sagiv, J. 1980. Organized Monolayers by adsorption. 1. Formation and structure of oleophobic mixed monolayers on solid surfaces. *J. Am. Chem. Soc.* 102:92–98.
14. Wu, E., K. Jacobson, and D. Papahadjopoulos. 1977. Lateral diffusion in phospholipid multilayers measured by fluorescence recovery after photobleaching. *Biochemistry.* 16:3936–3942.
15. Eagle, H. 1959. Amino acid metabolism in mammalian cell cultures. *Science (Wash. DC).* 130:432–437.
16. Kader, J. C., M. Julienne, and C. Vergnolle. 1984. Purification and characterization of a spinach-leaf protein capable of transferring phospholipids from liposomes to mitochondria or chloroplast. *Eur. J. Biochem.* 139:411–416.
17. Peters, R., A. Brunger, and K. Schulten. 1981. Continuous fluorescence microphotolysis: a sensitive method for study of diffusion processes in single cells. *Proc. Natl. Acad. Sci. USA.* 78:962–966.
18. Brunger, A., R. Peters, and K. Schulten. 1985. Continuous fluorescence microphotolysis to observe lateral diffusion in membranes. Theoretical methods and applications. *J. Chem. Phys.* 82:2147–2160.
19. Vincent, M., J. Gallay, J. de Bony, and J. F. Tocanne. 1985. Steady-state and time resolved fluorescence anisotropy study of phospholipid molecular motion in the gel phase using 1-palmitoyl-2-9-(2-anthryl)-nonanoyl-sn-glycero-3-phosphocholine. *Eur. J. Biochem.* 150:341–347.
20. Axelrod, D., D. E. Koppel, J. Schlessinger, E. Elson, and W. W. Webb. 1976. Mobility measurement by analysis of fluorescence photobleaching recovery kinetics. *Biophys. J.* 16:1055–1069.
21. Dahlquist, G., and G. Eriksson. 1983. Inverse non linear diffusion problem. Numerical treatment of inverses problems in differential and integral equation: Proceeding of an international workshop. Deuflhard and E. Hairer, editors. 238–245.
22. Ortega, J. M., and W. C. Rheinboldt. 1970. Iterative solution of non linear equations in several variables. *In* Computer Science and Scientific Computing. W. Rheinboldt, editor. Academic Press Inc., New York.
23. McGrath, A. E., C. G. Morgan, and G. K. Radda. 1976. Photobleaching. A novel fluorescence method for diffusion studies in lipid systems. *Biochim. Biophys. Acta.* 426:173–185.
24. Koppel, D. E., D. Axelrod, J. Schlessinger, E. L. Elson, and W. W. Webb. 1976. Dynamics of fluorescent marker concentration as a probe of mobility. *Biophys. J.* 16:1315–1329.
25. McConnell, H. M., T. H. Watts, R. M. Weis, and A. A. Brian. 1986. Supported planar membranes in studies of cell-cell recognition in the immune system. *Biochim. Biophys. Acta.* 864:95–106.
26. von Tscharner, V., and H. M. McConnell. 1981. Physical properties of lipid monolayers on alkylated planar glass surfaces. *Biophys. J.* 36:421–427.
27. Yechiel, E., and M. Edidin. 1987. Micrometer-scale domains in fibroblast plasma membranes. *J. Cell Biol.* 105:755–760.
28. Rimon, G., N. Meyersteim, and Y. I. Henis. 1984. Lateral mobility of phospholipids in the external and internal leaflets of normal and hereditary spherocytic human erythrocytes. *Biochim. Biophys. Acta.* 775:283–290.
29. Teissié, J., J. F. Tocanne, and A. Baudras. 1978. A fluorescence

approach of the determination of translational diffusion coefficients of lipids in phospholipid monolayers at the air water interface. *Eur. J. Biochem.* 83:77–85.

30. Theretz, A., J. Teissié, and J. F. Tocanne. 1984. A study of the structure and dynamics of complexes between polymyxin B and phosphatidylglycerol in monolayers by fluorescence. *Eur. J. Biochem.* 142:113–119.
31. Angelides, K. J., L. W. Elmer, D. Loftus, and E. Elson. 1988. Distribution and lateral mobility of voltage-dependent sodium channels in Neurons. *J. Cell Biol.* 106:1911–1925.